EurJIC
European Journal of Inorganic Chemistry

A Journal of
ChemPubSoc Europe

## Accepted Article

**Title:** Cu6S6 clusters as a building block for the stabilization of coordination polymers with NiAs, NaCl and related structures: synthesis, structure and catalytic studies

**Authors:** Srinivasan Natarajan and Ajay Kumar Jana

**To be cited as:** *Eur. J. Inorg. Chem.* 10.1002/ejic.201701262

**Link to VoR:** http://dx.doi.org/10.1002/ejic.201701262

WILEY-VCH

# $Cu_6S_6$ clusters as a building block for the stabilization of coordination polymers with NiAs, NaCl and related structures: synthesis, structure and catalytic studies

Ajay Kumar Jana[a] and Srinivasan Natarajan*[a]

**Abstract:** New three-dimensional heterometallic coordination polymers (CPs), $[\{Zn_3(Hen)(OH)\}\{Cu_6(6\text{-}mna)_6\}.(H_2O)_6]$, (**I**), $[\{Zn_2(OH)(en)\}\{Cu_6(6\text{-}mna)_6\}_{0.5}.(H_2O)_2.EtOH]$, (**II**), $[\{Zn_3(dap)_3(H_2O)\}\{Cu_6(6\text{-}mna)_6\}.(H_2O)_4]$, (**III**) and $[\{Zn_2(4,4'\text{-}bpy)_{0.5}(OH)(H_2O)\}\{Cu_6(6\text{-}mna)_6\}_{0.5}.(H_2O)]$, (**IV**), (en = ethylenediamine, 6-$H_2$mna = 6-mercaptonicotinic acid, dap = 1,2-diamino propane, 4,4'-bpy = 4,4'-bipyridine), were synthesized and their structures determined by single crystal X-ray crystallography. The structures of the compounds have $Cu_6S_6$ octahedral clusters linked through the carboxylates with different zinc-oxo clusters. The compounds have $Cu^{I}$ based clusters and $Zn^{II}$ based clusters, which are not observed commonly in coordination polymer structures. Compound **I** stabilizes in NiAs-related structure, compound **II** and **IV** in a NaCl related structure and compound **III** forms a new type of network structure. All the compounds were active for the heterogeneous nitroaldol reaction.

## Introduction

Inorganic-organic coordination polymer compounds, formed by the connectivity between the metal centers and bridging organic ligands, have been a topic of immense research during the last two decades.[1-5] The prospect of employing metal-oxo clusters instead of simple metal ions as part of this family of compounds have also been explored.[6-10] A prodigality of papers now exist where the metal-oxo clusters have been linked with organic ligands forming interesting structures.[11,12] During the last decade or so, the HSAB theory of Pearson[13] was utilized towards the design and synthesis of new coordination polymers.[14] A number of examples now exist where selective binding of metal ions were established based on some of the these ideas for successful design and synthesis of coordination polymers.

Over the years, many inorganic-organic coordination polymers have been prepared employing different metal clusters as the nodes.[15-19] For example, silver clusters such as $Ag_6S_6$, $Ag_9S_9$ etc. have been incorporated as part of the framework during the preparation of coordination polymer compounds.[20-25] We have been intrigued by the possibility of utilizing the ideas of HSAB theory towards the design of building units, which may lead to newer inorganic-organic coordination polymer compounds. To this end, we have employed the octahedral cluster, $Cu_6S_6$, as a building unit in preparing new compounds. It may be noted that the $Cu_6S_6$ cluster has been prepared earlier and employed as the building node for inorganic-organic coordination polymer compounds.[26,27] The $Cu_6S_6$ cluster has been prepared by reacting the soft acid $Cu^{1+}$ ions with soft bases such as –SH and –N present in the mercaptonicotinic acid.[26] It is known that the oxygens of the carboxylic acid is harder compare to the –SH and –N units. We wanted to explore the step-wise reaction in which the soft centers react first followed by reaction with hard centers. This approach was beneficial during our earlier studies with the $[Cu_6S_6]^{6-}$ cluster.[26] The previous work employed 2-mercaptonicotinic acid and in the present study the same cluster was prepared employing 6-mercaptonicotinic acid. This $Cu_6S_6$ cluster on reaction with $Zn^{2+}$ ions gave rise to four new compounds: $[\{Zn_3(Hen)(OH)\}\{Cu_6(6\text{-}mna)_6\}.(H_2O)_6]$, (**I**), $[\{Zn_2(OH)(en)\}\{Cu_6(6\text{-}mna)_6\}_{0.5}.(H_2O)_2.EtOH]$, (**II**), $[\{Zn_3(dap)_3(H_2O)\}\{Cu_6(6\text{-}mna)_6\}.(H_2O)_4]$, (**III**) and $[\{Zn_2(4,4'\text{-}bpy)_{0.5}(OH)(H_2O)\}\{Cu_6(6\text{-}mna)_6\}_{0.5}.(H_2O)]$, (**IV**). The heterometallic ($Cu^{1+}$ and $Zn^{2+}$ ions) coordination polymers have three-dimensional structures. In this manuscript, we present the synthesis, structure and the use of these compounds in heterogeneous catalytic nitroaldol reaction.

## Results and Discussion

The $Cu_6S_6$ cluster was prepared employing a reported procedure (see experimental section).[26] The heterometallic compounds, reported herein, were prepared by employing a three-layer approach. The first layer containing $Cu_6S_6$ was prepared by solubilizing the compound by employing bases such as ethylenediamine (en), 1,2-diaminopropane (dap), 4,4'-bipyridine and ammonium hydroxide. This solution was basic with a pH of 8.5. The secondary metal employed in the present study is zinc, which appear to form interesting open-framework structures under basic conditions exemplified by the preparation of a number of open-framework zinc-phosphates.[28-30] The basic pH may also prove beneficial in deprotonating the carboxylic acid and facilitating the binding of $Zn^{2+}$ ions with the carboxylate anions. In addition, we wanted to explore the possible importance of temperature in the synthesis of these compounds employing the layered approach. The usefulness of temperature in the bi-layer approach has been attempted before.[31] During the present study the layered reaction vessel was kept at 60°C and at 100°C (Table 4), which resulted in the compounds reported in this study. We also made attempts to prepare the present compounds without the layering approach, which resulted in mostly non-crystalline product. It is likely that the slow diffusion of the different ions helps in forming the products.

**Structure of $[\{Zn_3(Hen)(OH)\}\{Cu_6(6\text{-}mna)_6\}.(H_2O)_6]$, (I)** The asymmetric unit of **I** consists of six Cu(I), six 6-

---

[a] A. K. Jana, Prof. Dr. S. Natarajan
Framework Solids laboratory
Solid State and Structural Chemistry Unit
Indian Institute of Science, Bangalore–560012 (India)
Fax: (+91) 80-2361-1310
E-mail: snatarajan@.iisc.ac.in

Supporting information for this article is given via a link at the end of the document.

mercaptonicotinate ions, three $Zn^{2+}$ ions, one ethylene diamine, one hydroxyl group and six water molecules (Figure S1 in the Supporting Information). The copper atoms are coordinated by two sulfur atoms and one nitrogen atom forming a triangular coordination from three different 6-mercaptonicotinate ligands. The average Cu−N and Cu−S bond lengths are 2.017 Å and 2.252 Å, respectively (Table S1 in the Supporting Information). The distance between the two Cu(I) species within the $Cu_6$ cluster is in the range of 2.721(2) Å – 3.219(6) Å (Figure S2 in the Supporting Information). The $[Cu_6(6\text{-mna})_6]^{6-}$ cluster has six carboxylic acid groups; of which three carboxylate groups are connected with $Zn^{2+}$ ions via both the oxygen atoms and the other three carboxylates connect through one oxygen atom. This connectivity gives rise to a $\mu^{9}$-$\eta^{2}:\eta^{2}:\eta^{2}:\eta^{1}:\eta^{1}:\eta^{1}$ binding mode (Figure 1). Among the three $Zn^{2+}$ ions, Zn(1) and Zn(3) are tetrahedrally corordinated by three carboxylate oxygens and one hydroxyl group, whereas Zn(2) is octahedrally corordinated with three carboxylate oxygens, one hydroxyl group and two nitrogen atoms [N(7), N(8)] of the ethylene diamine molecule ( Figure S3 in the Supporting Information). The various bond distances and angles observed in **I** are within the expected ranges (Table S1 in the Supporting Information). It may be noted that the hydroxyl group (-OH) connects all the three zinc centers forming a $Zn_3$ trimer (Figure S4 in the Supporting Information). The various units would result in a formula, $[\{Zn_3(en)(OH)\}\{Cu_6(6\text{-mna})_6\}.(H_2O)_6]^{-}$, which is negatively charged. The negative charge is balanced by protonation of one of the nitrogen of the en molecule. We have employed a bond-valence sum calculation to ascertain the protonated nitrogen of the en molecule. Thus, from the bond valence sum calculation, atoms {N(7), N(8)}, it is likely that the N(8) would be protonated (Table S2 in the Supporting Information). The protonation of the nitrogen is also confirmed from the IR spectra, where a band at ~ 1451 $cm^{-1}$ is obtained, which corresponds to the asymmetric bending mode of the ammonium group.[32]

The structure of **I** can be considered to be built up from the connectivity between $Zn_3$ trimer units and $Cu_6$ octahedral units. Thus, the $Zn_3$ trimer units are connected with six different $[Cu_6(6\text{-mna})_6]^{6-}$ cluster units (Figure S5 in the Supporting Information). The $[Cu_6(6\text{-mna})_6]^{6-}$ cluster unit is also connected with six $Zn_3$ trimer units (Figure 1). Among the six carboxylate groups of the $[Cu_6(6\text{-mna})_6]^{6-}$ cluster, four caroboxylate groups connect with four $Zn_3$ trimer units in a plane forming a two dimensional sheet. The remaining carboxylate groups are connected with two $Zn_3$ trimer units from the adjacent layers above and below giving rise to the three dimensional structure (Figure 2).

To understand the structure better, we carried out a topological analysis using TOPOS.[33-35] Thus the $Zn_3$ trimer and $Cu_6(6\text{-mna})_6]^{6-}$ cluster were considered as two distinct nodes. This resulted in a 2-nodal net closely related to the NiAs structure (*nia* topology). The Schlafli symbol for this net is $(4^{12}.6^{3})(4^{9}.6^{6})$. Another way to interpret this net is to consider a hexagonal close packing (hcp) of $Zn_3$ units in which the octahedral voids are filled by the $Cu_6$ units. The structure contains a number of non-bonded extra-framework water molecules, which actively participate in hydrogen-bond interactions with the carboxylate oxygen atoms (Table S3 and Figure S6 in the supporting information).

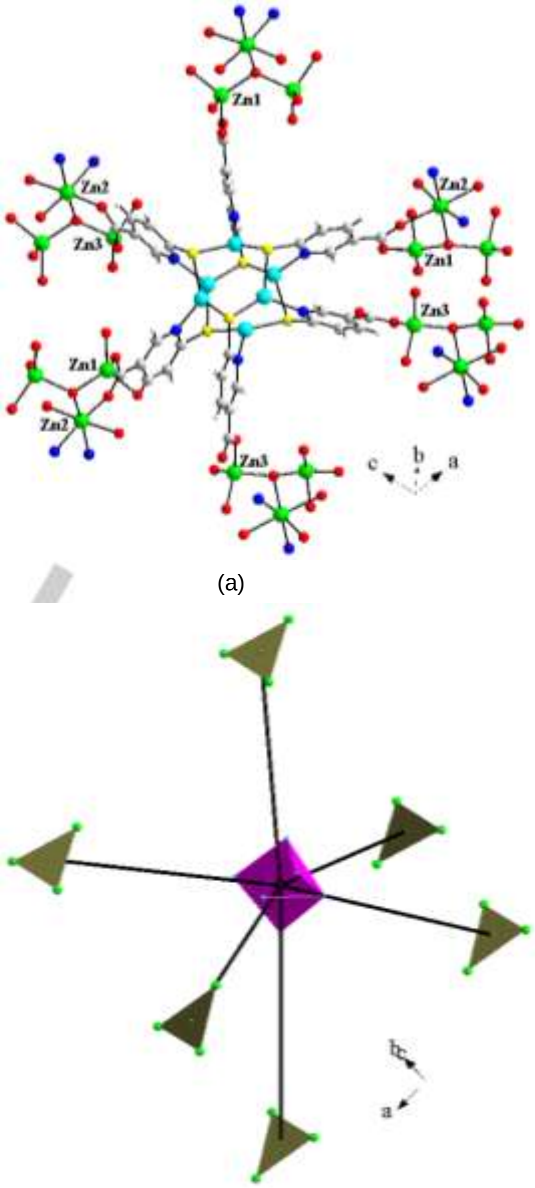

(a)

(b)

**Figure 1.** (a) The $[Cu_6(6\text{-mna})_6]^{6-}$ cluster and its connectivity with the $Zn_3$ cluster in **I**. (b) The $[Cu_6(6\text{-mna})_6]^{6-}$ cluster (pink) octahedral cluster and the $Zn_3$ trimer cluster (brown) and their connectivity. Note that the $Cu_6S_6$ cluster connect with four $Zn_3$ trimers in-plane and two $Zn_3$ trimers out-of-plane (see text).

### Structure of $[\{Zn_2(OH)(en)\}\{Cu_6(6\text{-mna})_6\}_{0.5}.(H_2O)_2.EtOH]$, (II)

The asymmetric unit of **II** consists of three Cu(I), three 6-mercaptonicotinate ions, two $Zn^{2+}$ ions, one ethylene diamine, one ethanol, one hydroxyl ion and two water molecules (Figure S7 in the Supporting Information). Similar to the structure of **I**, the octahedral $[Cu_6(6\text{-mna})_6]^{6-}$ cluster was formed by the connectivity between sulfur and nitrogen atoms from the mercaptonicotinate anions. The Cu(I) has a triangular coordination formed by two sulfur atoms and one nitrogen atom from three 6-mercaptonicotinate units, with average Cu−N and

Cu−S bond lengths of 2.019 Å and 2.244 Å, respectively (Table S1 in the Supporting Information). The Cu(I) atoms, within the cluster, are separated from each other with distances in the range of 2.674(3) Å - 3.313(1) Å (Figure S8 in the Supporting Information). Of the six carboxylate units of the $[Cu_6(6\text{-mna})_6]^{6-}$ cluster, four are bound with eight $Zn^{2+}$ ions through both the oxygen atoms, while the other two connect with two $Zn^{2+}$ ions through one oxygen atom. This connectivity gives rise to a $\mu^{10}$-$\eta^2$:$\eta^2$:$\eta^2$:$\eta^2$:$\eta^1$:$\eta^1$ binding mode (Figure 3). Of the two $Zn^{2+}$ ions, Zn(1) is octahedrally corordinated with two carboxylate oxygen [O(4), O(6)], two hydroxyl oxygens [O(7), O(7a)] and two nitrogen [N(4), N(5)] from the ethylenediamine molecule; and Zn(2) is tetrahedrally corordinated with three carboxylate oxygen [O(2), O(3), O(5)] and one hydroxyl oxygen [O(7)] ( Figure S9 in the Supporting Information). The Zn(1) and Zn(2) atoms are connected through the hydroxyl oxygens [O(7)] forming a $Zn_4$ tetramer unit (Figure S10 in the Supporting Information).

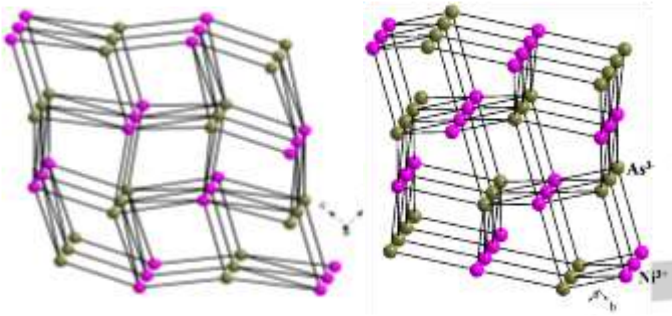

(a) (b)

**Figure 2**. (a) Figure shows the three-dimensional connectivity in **I**. The $Cu_6S_6$ cluster (pink) and the $Zn_3$ trimer (brown). (b) The NiAs structure. Note the close similarity between the two structures (Ni ≡ $Cu_6S_6$, As ≡ $Zn_3$).

Similar to the structure of **I**, we can understand this structure also by considering the connectivity between the $Zn_4$ tetramer units and the $Cu_6$ octahedral units. Thus, the $Zn_4$ tetramer units are connected with six different $[Cu_6(6\text{-mna})_6]^{6-}$ clusters (Figure 4). Similarly each $[Cu_6(6\text{-mna})_6]^{6-}$ cluster unit is also connected with six $Zn_4$ tetramer units (Figure 3). It may be noted that four carboxylate units bind with four $Zn_4$ tetramer units within a plane forming a two dimensional layer like arrangement. The other two carboxylate groups connect with $Zn_4$ tetramer units of the adjacent layer on both the sides. This connectivity results in a 6:6 binding between the $Zn_4$ tetramer and the $Cu_6S_6$ octahedral cluster. A close examination of this bonding reveals a resemblance to the three dimensional NaCl - like structure (Figure 5). To understand the structure further, we have carried out the TOPOS analysis.[33-35] For the topological analysis, the $Zn_4$ tetramer and $[Cu_6(6\text{-mna})_6]^{6-}$ cluster units were considered as two distinct nodes. This resulted in an uninodal net; with a *α-Po* topology. The Schlafli symbol for this net is $(4^{12}.6^3)$. The guest molecules, water and ethanol participates in hydrogen-bond interactions (Table S3 and Figure S11 in the supporting information).

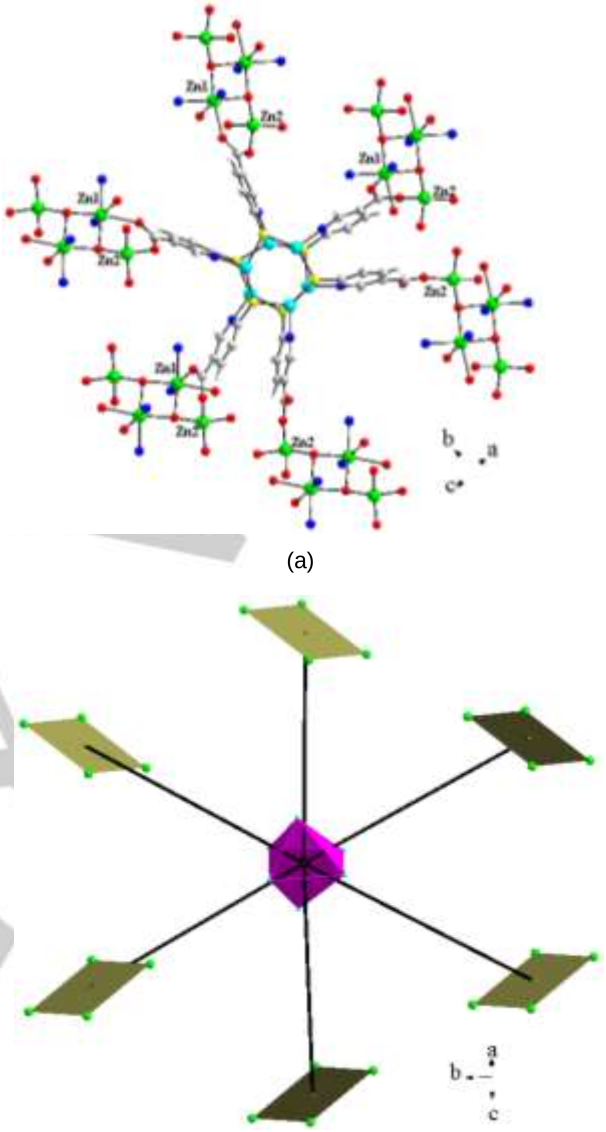

(a)

(b)

**Figure 3.** (a) The $[Cu_6(6\text{-mna})_6]^{6-}$ cluster and its connectivity with $Zn_4$ tetramers in **II**. (b) The octahedral $Cu_6S_6$ cluster (pink) and the $Zn_4$ tetramer (brown) connectivity in **II**. Note that the octahedral $Cu_6S_6$ cluster connects with six $Zn_4$ tetramers (see text).

**Structure of $[\{Zn_3(dap)_3(H_2O)\}\{Cu_6(6\text{-mna})_6\}.(H_2O)_4]$, (III)** The asymmetric unit consists of six Cu(I), six 6-mercaptonicotinate ions, three $Zn^{2+}$ ions, three 1,2-diaminopropane and five water molecules (Figure S12 in the Supporting Information). The structure contains two independent $[Cu_6(6\text{-mna})_6]^{6-}$ cluster units: 2 x Cu(1), Cu(2), Cu(3) (cluster-1) and 2 x Cu(4), Cu(5), Cu(6) (cluster-2). Similar to the previous structures, the copper atoms have the trigonal coordination formed by two sulfur atoms and one nitrogen atom from three 6-mercaptonicotinate ligands (Table S1 in the Supporting Information). The Cu-atoms within the cluster are separated from each other with distances in the range 2.729(4)Å – 3.076(7) Å (Figure S13 in the Supporting Information).

10.1002/ejic.201701262

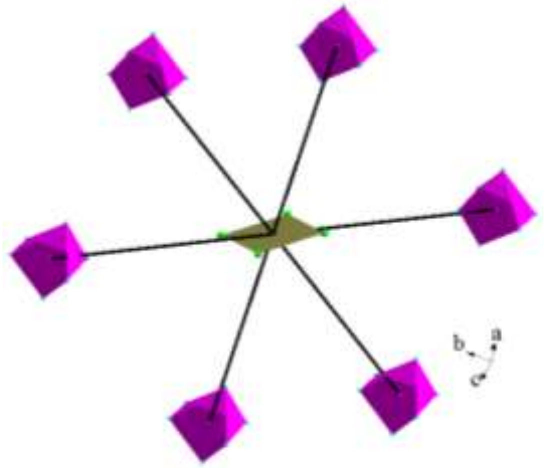

**Figure 4.** The Zn$_4$ tetramer (brown) connectivity with Cu$_6$S$_6$ cluster (pink). Note that the Zn$_4$ tetramer connects with six Cu$_6$S$_6$ cluster (see text).

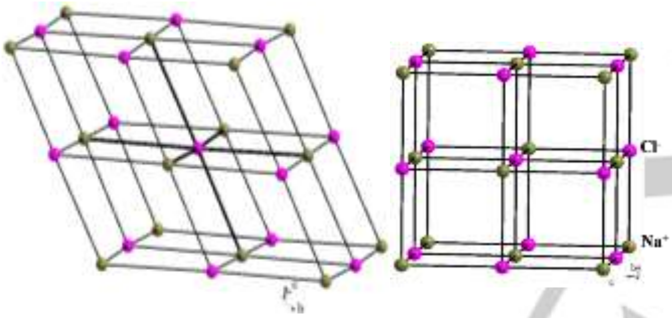

(a) (b)

**Figure 5.** (a) Three dimensional connectivity between Cu$_6$S$_6$ cluster (pink) and Zn$_4$ tetramers (brown). (b) The NaCl structure. Note the close similarly between the structures (see text).

Among the three Zn$^{2+}$ ions, Zn(1) and Zn(3) are tetrahedrally corordinated with two carboxylate oxygens and two nitrogen from the 1,2-diaminopropane molecule (Figure S14-S15 in the Supporting Information) and Zn(2) has a distorted trigonal bipyramidal geometry from two carboxylate oxygens [O(3), O(5)], one water molecule [O(13)] and two nitrogen atoms from the 1,2-diaminopropane molecule (Figure S16 in the Supporting Information). The geometry of the Zn(2) ions was determined by employing the method described by earlier.[36] The parameter, τ, suggests the possible geometry for the central metal ion. Thus, τ = 1 for a perfect trigonal bipyramidal geometry and τ = 0 for a perfect square pyramidal geometry. The value of τ parameter was found 0.52 for Zn(2), which indicates that geometry around Zn(2) ion is a highly distorted. The connectivity between the three Zn$^{2+}$ ions and the octahedral [Cu$_6$(6-mna)$_6$]$^{6-}$ clusters are similar. Thus, cluster-1 binds with four Zn(2) ions and two Zn(1) ions while cluster-2 binds with four Zn(3) ions and two Zn(1) ions through the mono-dentate coordination of the carboxylate unit (Figure 7). This binding gives rise to a $\mu^{6}\text{-}\eta^{1}:\eta^{1}:\eta^{1}:\eta^{1}:\eta^{1}:\eta^{1}$ binding mode (Figure 6). The structure of **III** can be understood better by considering individual connectivities of each Cu$_6$ cluster. Thus cluster-1 connects with four Zn(2) ions to form a one-dimensional chain like arrangement. Similarly, cluster-2 connects with four Zn(3) ions forming a one-dimensional arrangement (Figure 7). The two chain structures are cross-linked by Zn(1) ion forming the extended three-dimensional structure (Figure 8). Though the connectivity appears simple, the relative disposition of the independent copper cluster-Zn chain units make the understanding of the structure difficult. To have a better understanding of the structure, TOPOS analysis with the three Zn centers (Zn1, Zn2 and Zn3) as well as cluster-1 and cluster-2 as independent nodes were considered. The TOPOS analysis gave a new topology with Schlafli symbol of (12) $(4^{2}.12^{9}.16^{4})$ $(4)^{2}$. The presence of a number of extra-framework water molecules gives rise to hydrogen-bond interactions (Table S3 and Figure S17 in the supporting information).

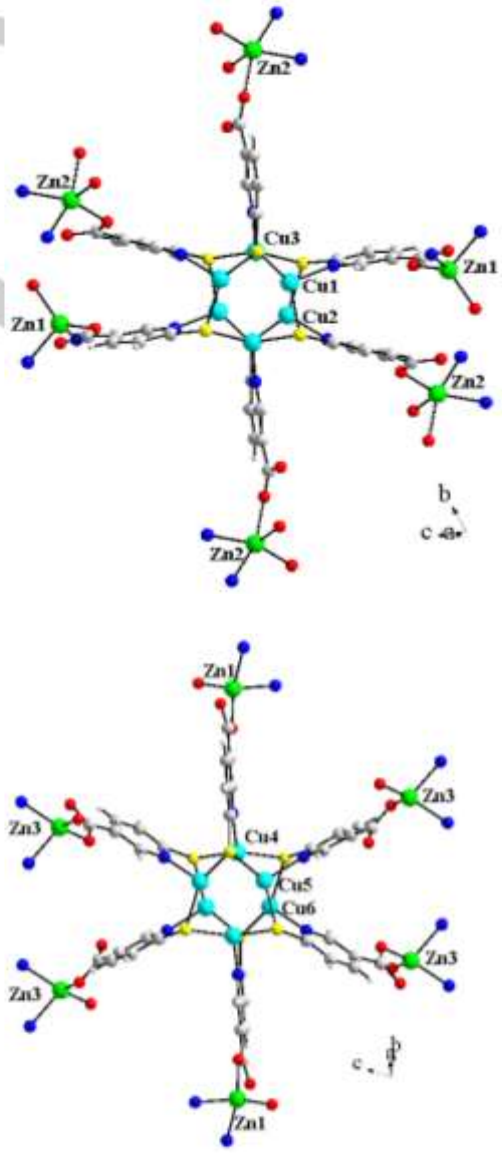

**Figure 6.** The two [Cu$_6$(6-mna)$_6$]$^{6-}$ clusters and their connectivity with the Zn in **III**.

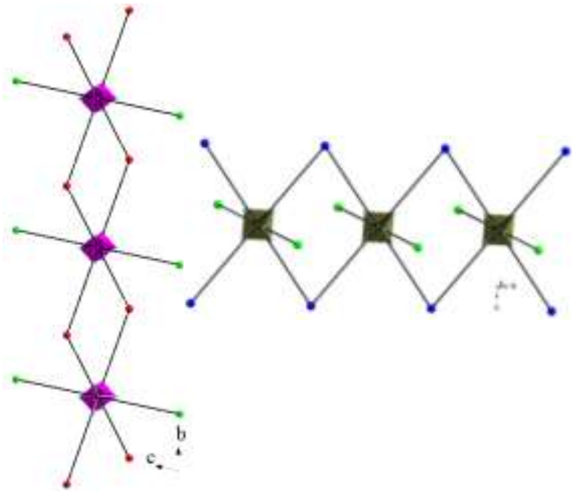

(a) (b)

**Figure 7.** (a) Figure shows the connectivity between [$Cu_6S_6$] cluster and Zn atoms forming a one-dimensional chain. (b) Similar connectivity involving cluster-2.

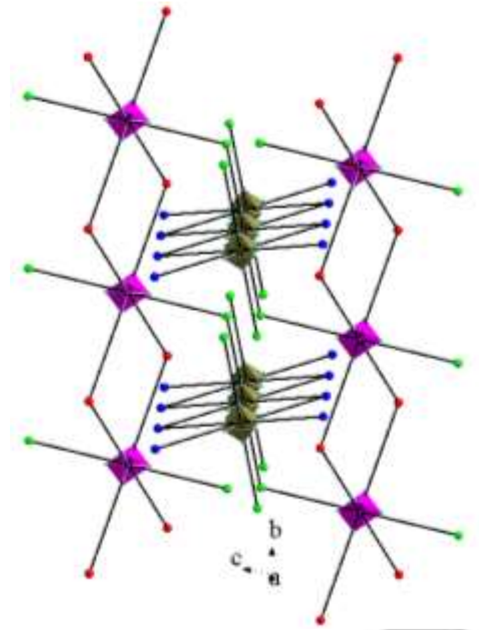

**Figure 8.** The connectivity between the two chain structures through the Zn(1) (green). Note that the chains are not parallel to each other (see text).

**Structure of [{$Zn_2$(4,4'-bpy)$_{0.5}$(OH)($H_2O$)}{$Cu_6$(6-mna)$_6$}$_{0.5}$.($H_2O$)], (IV)** The asymmetric unit consists of three Cu(I), three 6-mercaptonicotinate ions, two $Zn^{2+}$ ions, one lattice water, one coordinated water, one hydroxyl ion and half 4,4'-bipyridine ligand (Figure S18 in the Supporting Information). The Cu(I) centers have a trigonal coordination (Table S1 in the Supporting Information) and the Cu-Cu distances within the $Cu_6$ octahedral cluster are in the range of 2.793(5) Å - 3.501(11) Å (Figure S19 in the Supporting Information). Of the six carboxylate units attached with the [$Cu_6$(6-mna)$_6$]$^{6-}$ cluster, four bonds with eight $Zn^{2+}$ ions via both the oxygen atoms and two carboxylates connect to two $Zn^{2+}$ ions via one oxygen atom. This connectivity gives rise to $\mu^{10}$-$\eta^2$:$\eta^2$:$\eta^2$:$\eta^2$:$\eta^1$:$\eta^1$ binding mode (Figure 9). Of the two $Zn^{2+}$ ions, Zn(1) has a tetrahedral coordination and Zn(2) is octahedrally coordinated. The zinc ions are connected through the hydroxyl oxygen [O(7)] forming a $Zn_4$ tetramer (Figure S20 in the Supporting Information). This $Zn_4$ tetramer closely resembles the $Zn_4$ tetramer units observed in **II** (Figure S21 in the Supporting Information).

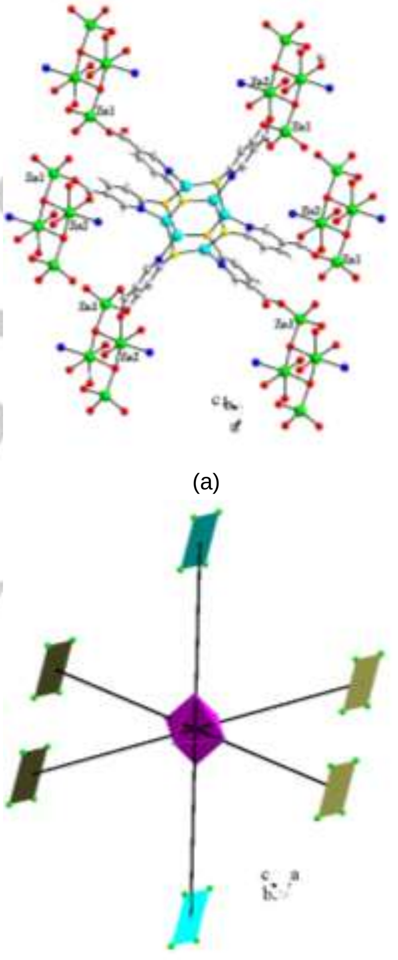

(a)

(b)

**Figure 9.** (a) The connectivity between [$Cu_6$(6-mna)$_6$]$^{6-}$ cluster and $Zn_4$ tetramer units in **IV**. (b) The octahedral $Cu_6S_6$ cluster (pink) and the $Zn_4$ tetramer (brown, in-plane; cyan, out-of-plane) connectivity in **IV**. Note that the octahedral $Cu_6S_6$ cluster connects with six $Zn_4$ tetramers.

The $Cu_6$ octahedral clusters and the $Zn_4$ tetramer units are connected together forming the structure of **IV**. The $Zn_4$ tetramer units are connected with six carboxylate units from six different [$Cu_6$(6-mna)$_6$]$^{6-}$ clusters. The 4,4'-bipyridine ligand links the $Zn_4$ tetramers along the [020] direction (Figure 10). The [$Cu_6$(6-mna)$_6$]$^{6-}$ cluster units are also connected with six $Zn_4$ tetramer units (Figure S22 in the Supporting Information). The connectivity between $Cu_6$ cluster units and $Zn_4$ tetramer units are similar to that observed in the structure of **II**. Thus, four $Zn_4$ tetramer units bind with four carboxylates of $Cu_6$ clusters within the plane and two carboxylate units connect with $Zn_4$ tetramer units present in adjacent layers giving rise to the three-dimensional structure

(Figure S23 in the Supporting Information). Thus the structure of **IV** also has a 6:6 connectivity between the $Cu_6$ and $Zn_4$ units. The presence of 4,4'-bipyridine and its connection with $Zn_4$ tetramer, however adds an additional twist to the structure. A TOPOS[33-35] analysis with the $Zn_4$ tetramer and $Cu_6(6\text{-mna})_6]^{6-}$ cluster as two different nodes results in a uninodal *α-Po* topology. If the 4,4'-bipyridine link between the Zn-center is also considered, a new topology would result. The Schlafli symbol for this new net would be $(3^2.4^{10}.5^2.6)(3^4.4^{12}.5^8.6^4)$. The extra-framework water molecule, participates in hydrogen-bond interactions (Table S3 and Figure S24 in the supporting information).

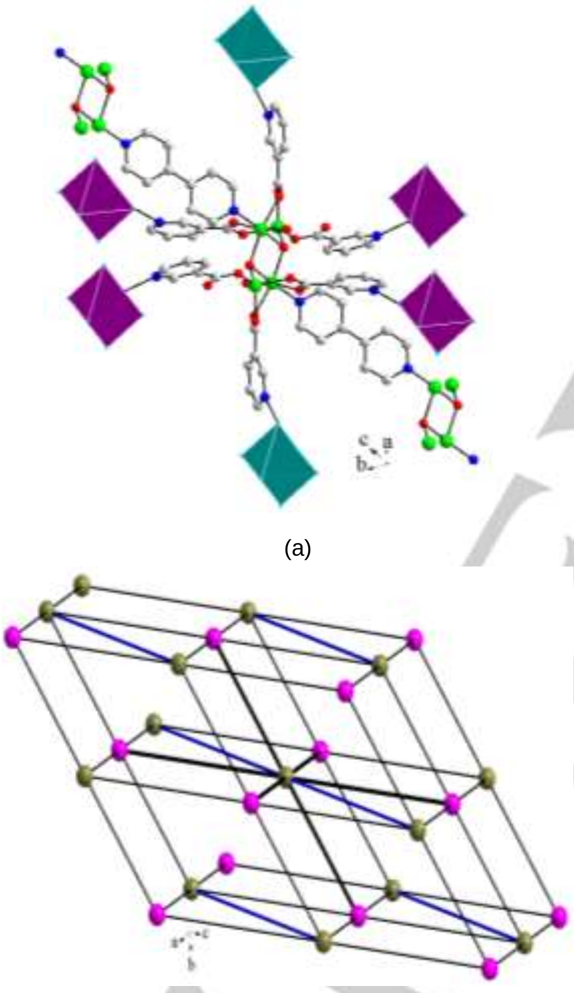
(a)

(b)

**Figure 10.** (a) Figure shows the $Zn_4$ tetramer connectivity with $Cu_6S_6$ cluster. Note that four $Cu_6S_6$ clusters connect in-plane (pink) and two $Cu_6S_6$ clusters out-of-plane (cyan). Note also that the 4,4'-bipyridine unit connects two $Zn_4$ tetramers. (b) The structure of **IV** showing the connectivity between octahedral $Cu_6S_6$ (pink) and $Zn_4$ tetramer (brown). The blue line represents connectivity involving the 4,4'-bipyridine moiety. Note the close similarity to structure of **II** and NaCl structure (Figure 5b).

**Structural comparison:** From the synthesis conditions, the longer duration of the reaction time forms a structure that is more stable. The synthesis conditions for **I** and **II** are similar but during the formation of **II**, the reaction mixture was allowed to react for 96h at 100°C. As described above, compound **I** stabilized in NiAs-related structure whereas compound **II** stabilizes in NaCl-related structure. From the solid state chemistry point of view, the NaCl structure is more stable compared to NiAs structure.[37] Similarly, it is likely that the longer duration of the reaction gave rise to a thermodynamically more stable phase in **II** (NaCl-related) compared to **I** (NiAs-related). Similarly, in the formation of **IV** also one can make such observation. The presence of 4,4'-bipyridine actually links two Zn-centers creating a disruption in the overall structure, though the overall topology is NaCl-related. The new network observed for **III** could be due to the shorter duration as well as lower temperature. It has been established both in framework compounds such as zeolites, aluminophosphates etc[38] and inorganic-organic hybrids[39] that higher temperature and / or longer duration during the synthesis results in dense framework that are thermodynamically stable.

As mentioned earlier, the $Cu_6S_6$ octahedral units have been stabilized before by the use of other ligands.[26,27] As part of the present study, we have employed the $[Cu_6(mna)_6]^{6-}$ ions as a ligand to react with a secondary metal ion ($Zn^{2+}$ ion) to convert the molecular structure of $[Cu_6(mna)_6]$ clusters into three-dimensional ones. Thus, four new $Cu^{1+}$-$Zn^{2+}$ heterometallic compounds with three – dimensional structures have been isolated. In an earlier study, we employed $Mn^{2+}$ ions as the secondary metal ions to stabilize the $[Cu_6(mna)_6]^{6-}$ clusters into extended structures.[26] It is interesting to note that the presence of M (M = Mn, Zn) tetramer clusters appear to form a 6:6 connectivity with the $[Cu_6(mna)_6]^{6-}$ clusters giving rise to a α-Po (NaCl-related) structure. A similar observation was also made with $[Ag_6(mna)_6]^{6-}$ cluster with $Na^+$ ions in $4Na^+.2[C_4O_3H_{12}N]^+.[Ag_6(mna)_6]^{6-}.10H_2O$.[40] The connectivity between $[Ag_6(mna)_6]^{6-}$ clusters with alkaline earth metal ions (Ca, Sr, Ba), on the other hand, forms many different structures.[25] Of these, the connectivity involving $Sr_2$ dimers and $Sr_4$ tetramers with $[Ag_6(mna)_6]^{6-}$ gives rise to the α-Po structure (Figure 11). It appears that the octahedral molecular clusters $[Cu_6(mna)_6]^{6-}$ and $[Ag_6(mna)_6]^{6-}$ are versatile binding units for the preparation of new inorganic coordination polymers.

### The thermogravimetric analysis (TGA):

The thermogravimetric analysis (TGA) studies were carried out in the temperature range of 30 - 900°C (heating rate = 10°C $min^{-1}$) under a flowing $N_2$ atmosphere (40 mL $min^{-1}$) (Figure 12). For compound **I**, a weight loss of ~10.6% was observed in the temperature range of 30-250°C. This would correspond to the loss of seven water molecules and one ethylenediamine molecule (cal. 11.1%). The broad weight loss in the temperature range of 250-730°C was found to be ~ 55.8%, which corresponds to the loss of six mercaptonicotinate moieties (cal. 55%). For compound **II**, the observed weight loss in the temperature range of 30-340°C was 21.7%, which corresponds to the loss of two water molecules, one hydroxyl ion, one ethanol

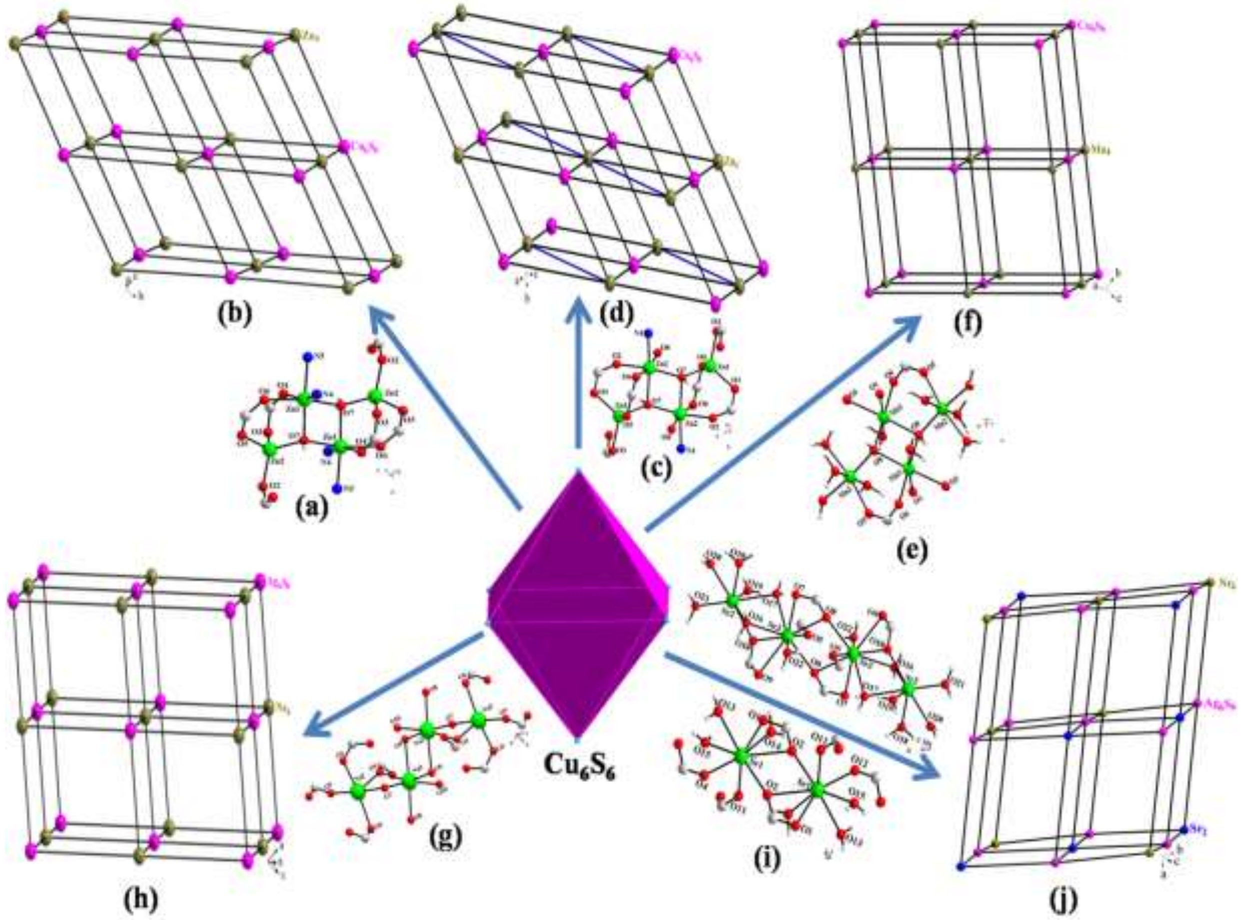

**Figure 11.** (a) Comparison of structures involving octahedral $Cu_6$ or $Ag_6$ clusters and different metal-oxo clusters. (a) $Zn_4$ tetramer in **II**, (c) $Zn_4$ tetramer in **IV**, (e) $Mn_4$ tetramer in Ref. 26, (g) $Na_4$ tetramer in Ref. 40, (i) $Sr_2$ dimer and $Sr_4$ tetramer in Ref. 25; The node representation of the observed structures (b) in **II**, (d) in **IV**, (f) in Ref. 26, (h) in Ref. 40, (j) in Ref. 25 respectively.

molecule and one ethylenediamine molecule (cal. 16.9%). The observed weight loss in the temperature range 340-715°C was 46.2%, which corresponds to the loss of three mercaptonicotinate moieties (cal. 48.9%). For compound **III**, in the temperature range of 30-260°C, the observed weight loss was 5.9%, which corresponds to the loss of one coordinated water and four lattice water molecules (cal. 4.98%). The second weight loss in the temperature range of 260-720°C was found to be ~58.1%, which corresponds to the loss of three 1,2-diaminopropane molecules and six mercaptonicotinate moieties (cal. 63.1%). For compound **IV**, in the temperature range 30-350°C, the observed weight loss 9.9%, which corresponds to the loss of one lattice water molecule, one coordinated water molecule and the 4,4'-bipyridine moiety (cal. 12.5%). The weight loss in the temperature range 350-780°C was ~ 53.1%, which corresponds to the loss of three mercaptonicotinate moities (cal. 50.3%). The TGA results are represented in Table 1. The calcined compound, after TGA studies in all the case was a mixture of CuO and ZnO (JCPDS No: 89-5895 and 89-1397) (Figure S25 in the Supporting Information).

### Nitroaldol reaction:

The Nitroaldol or Henry reaction is an important C-C bond coupling reactions employing nitroalkane and aldehyde.[41-54] We desired to explore this reaction employing the present compounds as heterogeneous catalysts. Previous studies suggested that the tetrahedral $Zn^{2+}$ ions may act as a Lewis acid center catalyzing this reaction.[46-54] In the present study, all the four compounds have tetrahedral Zn(II) ions as part of the structure and it occurred to us that the present compounds could also be active for the nitroaldol reaction. Thus, the catalytic activities of all the compounds (**I–IV**) were examined using nitromethane along with different aldehydes. The products of the reaction were characterized by $^1$H-NMR spectroscopy.[52,53] In all the cases, the reaction proceeded as expected and the yield of the reaction varied from 41-94%. The yield appears to depend on the aldehyde employed in the reaction (Table 2). The yield was higher when electronegative groups are present as part of the aromatic ring of the aldehyde. It is likely that the electronegative groups stabilizes the transition state of the reaction (Scheme 1).[47]

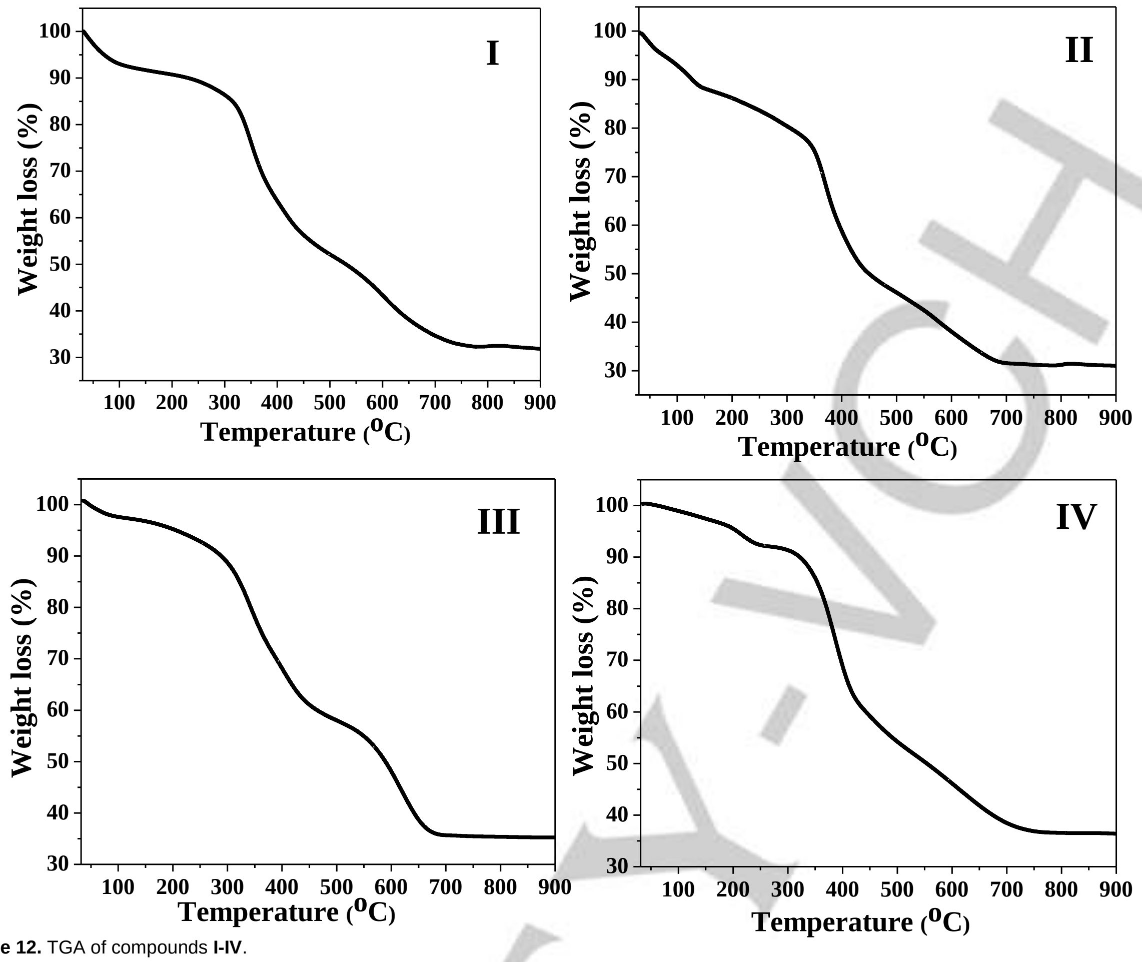

**Figure 12.** TGA of compounds **I-IV**.

**Table 1.** The results for the TGA studies for compounds **I-IV**.

| Compound | Temperature range (°C) | Weight loss (%) | | Possible loss |
|---|---|---|---|---|
| | | Observed | Calculated | |
| [{$Zn_3$(Hen)(OH)}{$Cu_6$(6-mna)$_6$}.($H_2O$)$_6$], (**I**) | 30-250 | 10.6 | 11.1 | 6$H_2O$ and one ethylenediamine (en) |
| | 250-730 | 55.8 | 55 | six mercaptonicotinate moieties |
| [{$Zn_2$(OH)(en)}{$Cu_6$(6-mna)$_6$}$_{0.5}$.($H_2O$)$_2$.EtOH], (**II**) | 30-340 | 21.7 | 16.9 | 2$H_2O$, $OH^-$, EtOH, en |
| | 340-715 | 46.2 | 48.9 | three mercaptonicotinate moieties |
| [{$Zn_3$(dap)$_3$($H_2O$)}{$Cu_6$(6-mna)$_6$}.($H_2O$)$_4$], (**III**) | 30-260 | 5.9 | 4.98 | 5$H_2O$ |
| | 260-720 | 58.1 | 63.1 | three 1,2-diaminopropane molecules and six mercaptonicotinate moieties |
| [{$Zn_2$(4,4'-bpy)$_{0.5}$(OH) ($H_2O$)}{$Cu_6$(6-mna)$_6$}$_{0.5}$. ($H_2O$)], (**IV**) | 30-350 | 9.9 | 12.5 | 2$H_2O$ and the 4,4'-bipyridine moiety |
| | 350-780 | 53.1 | 50.3 | three mercaptonicotinate moities |

The tetrahedrally coordinated Zn(II) ions indeed act as a Lewis acid center by accepting the lone pair of electrons from the oxygen atom of the aldehyde as well as the electron density from the nitro group of nitromethane (Scheme 1B). The catalytic activities and yield of the products observed employing the present compounds are comparable with those reported in the literature (Table 3).[49-54] In order to investigate the possible reuse of the catalyst, we isolated the catalyst after the reaction and reemployed for the same reaction for up to 3 cycles. The re-used catalyst exhibits comparable activity with reasonable yields of 71% (Figure 13).

We have also carried out the reaction between benzaldehyde and nitromethane in the absence of the present compounds as well as in the presence of $ZnCl_2$, $Zn(NO_3)_2$ and free metalloligand [$Cu_6(Hmna)_6$]. In all the cases, we did not observe the formation of the desired nitroaldol product. This suggests that the present compounds act heterogeneous catalyst for this reaction. We examined the structural integrity of the catalyst during the repeated use. The PXRD pattern indicated that the structural integrity of the compound remains the same after 3-cycles (Figure S26-S27 in the Supporting Information).

**Table 2.** Nitroaldol reaction between aromatic aldehyde and nitromethane employing **I-IV** as a catalyst.

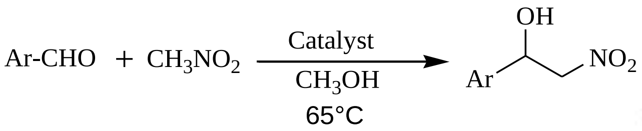

| Entry | Substrate | Reaction time (h) | Product | Yield % | | | |
|---|---|---|---|---|---|---|---|
| | | | | I | II | III | IV |
| 1 | 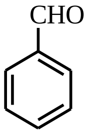 | 48 | 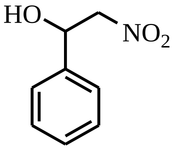 | 72 | 63 | 78 | 42 |
| 2 | 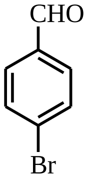 | 24 | 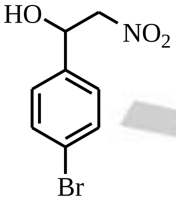 | 79 | 68 | 76 | 51 |
| 3 | 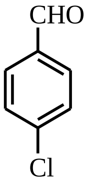 | 24 | 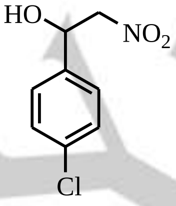 | 81 | 70 | 75 | 44 |
| 4 | 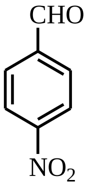 | 24 | 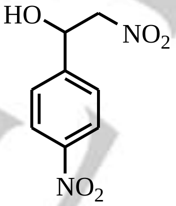 | 92 | 81 | 94 | 56 |
| 5 | 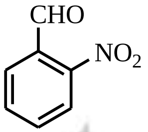 | 24 | 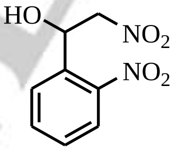 | 84 | 76 | 82 | 54 |
| 6 | 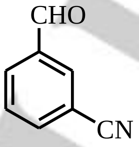 | 24 | 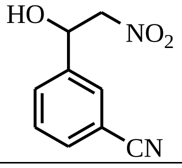 | 78 | 62 | 68 | 41 |

Reaction conditions: Aromatic aldehyde (0.5 mmol), nitromethane (1.5 mmol), MeOH (2.5 mL), and catalyst (10 mol %). Yield based on column chromatography.

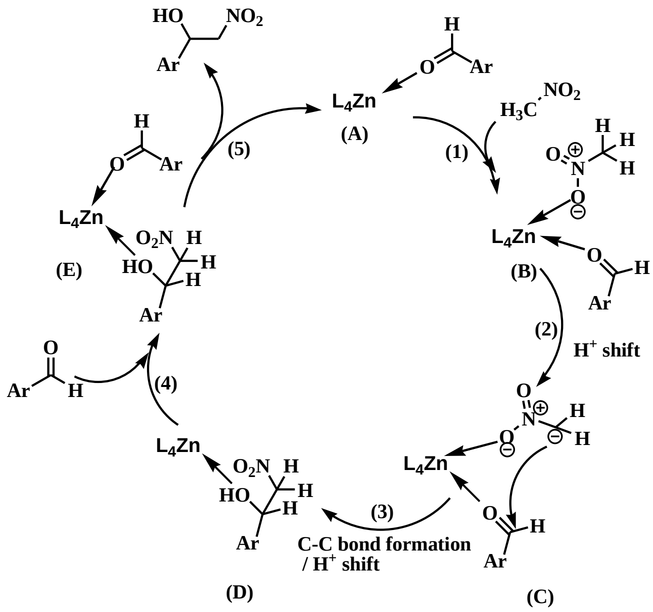

Scheme 1. The proposed mechanism of nitroaldol reaction.

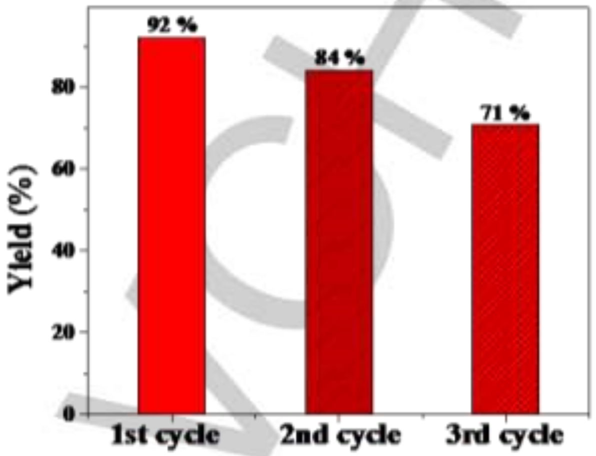

**Figure 13.** The yield for recyclability test up to 3rd cycles using compound-**I** as a catalyst.

**Table 3.** Nitroaldol reaction between aryl aldehyde and nitromethane catalyzed by Zn(II) based catalysts reported in the literature.

| Aryl aldehyde | Catalyst | Reaction conditions | % Yield | Ref. |
|---|---|---|---|---|
| Benzaldehyde | Zn(**L**)Cl$_2$ | MeOH/25°C/7d/10 mol% | 55 | 49 |
| 4-Nitrobenzaldehyde | Zn-MOF **1** | CH$_3$NO$_2$/60°C/120h/1.6 mol% | 80 | 50 |
| 4-Chlorobenzaldehyde | ZnLs | EtOH/25°C/5h/10 mol% | 85 | 51 |
| 4-Nitrobenzaldehyde | ZnLs | EtOH/25°C/5h/10 mol% | 96 | 51 |
| Benzaldehyde | Zinc-Fam Catalyst | THF/-50°C/24h/54 mol% | 83 | 52 |
| 4-Nitrobenzaldehyde | Zinc-Fam Catalyst | THF/-50°C/24h/54 mol% | 84 | 52 |
| 4-Bromobenzaldehyde | Zinc-Fam Catalyst | THF/-50°C/24h/54 mol% | 73 | 52 |
| Benzaldehyde | Et$_2$Zn/**1f** | THF/-35°C/24h/10 mol% | 52 | 53 |
| Benzaldehyde | Zn Catalyst (**2**) | THF/-35°C/24h/5 mol% | 75 | 54 |
| 1-Naphthaldehyde | Zn Catalyst (**2**) | THF/-35°C/24h/5 mol% | 71 | 54 |
| Benzaldehyde | Compound-**I** | MeOH/65°C/48h/10 mol% | 72 | This study |
| 4-Nitrobenzaldehyde | Compound-**III** | MeOH/65°C/24h/10 mol% | 94 | This study |

## Conclusions

The synthesis, structure and heterogeneous catalytic activity of four three-dimensional heterometallic coordination polymer compounds have been accomplished. All the compounds have $Cu_6S_6$ octahedral clusters connected with different Zn-oxo clusters forming the extended 3D structures. The $Cu_6S_6$ octahedral cluster appears to be a versatile building block in forming newer assemblies. In the present study, we stabilized the $Cu_6S_6$ cluster in NiAs-related (**I**) and NaCl-related structures (**II** and **IV**) along with a new type of network structure (**III**). We have earlier reported a NaCl network structure based on $Cu_6S_6$ cluster in {[$Mn_4(OH)_2(H_2O)_{10}$][($Cu_6$(2-mna)$_6$]·8$H_2O$}[26] and {[$Sr_3(H_2O)_{10}$][$Ag_6$(2-mna)$_6$]·12$H_2O$}.[25] The Lewis acid nitroaldol reactions were shown to be promoted by these compounds with very good catalytic activity. From the present study, it is clear that the [$Cu_6$(mna)$_6$] is a good building block to investigate with many other elements as the softer –SH and –N were employed first to stabilize the $Cu_6S_6$ cluster. The number of hard acids such as $Fe^{2+}$/$Al^{3+}$ etc can also be attempted to form new type of extended structures. Studies towards this goal are being perused and the results would be reported in future.

## Experimental Section

**Materials:** 6-mercaptonicotinic acid was acquired from Sigma-Aldrich. CuI, 4,4'-bipyridine, N,N'-dimethylformamide, $Zn(NO_3)_2.6H_2O$, $Zn(OAc)_2.2H_2O$, EtOH, ethylenediamine, 1,2-diaminopropane nitromethane, methanol, benzaldehyde, 4-bromobenzaldehyde, 4-chlorobenzaldehyde, 4-nitrobenzaldehyde, 2-nitrobenzaldehyde, 3-cyanobenzaldehyde were obtained from SDfine (India). All the chemicals are used without further purification.

**Synthesis:**

**Preparation of $[Cu_6(6\text{-}Hmna)_6]$ metalloligand:** We have earlier prepared the metalloligand, $[Cu_6(2\text{-}Hmna)_6]$.[26] We have adopted the same procedure for the synthesis of $[Cu_6(6\text{-}Hmna)_6]$ metalloligand. In a typical procedure, a mixture of CuI (0.019 g, 0.1 mmol), 6–mercaptonicotinic acid (0.031 g, 0.1 mmol) in 1 mL of water were sonicated at room temperature for 15 min. After the sonication bright orange colored precipitate was observed, which was dissolved by adding appropriate bases (for **I** and **II**: ethylenediamine, for **III**: 1,2-diaminopropane, for **IV**: 4,4'-bipyridine and aqueous $NH_3$). The resulting orange colored solution was employed for the preparation of the compounds reported in this paper.

**Synthesis of $[\{Zn_3(Hen)(OH)\}\{Cu_6(6\text{-}mna)_6\}.(H_2O)_6]$, (I):** In a 6 mL test tube 1mL of the metalloligand solution (ethylene diamine as the base) was taken and 1:1 water/ethanol mixture (1mL) was carefully layered on top. A solution containing $Zn(NO_3)_2.6H_2O$ (0.03 g, 0.1 mmol) in 1 mL ethanol was layered on top of the water/ethanol mixture. The test tube was carefully sealed by a screw cap and the reaction vessel was kept at 100°C. After two days, we observed the formation of brown colored rod-shaped crystals (Figure S28 in the Supporting Information), which were carefully harvested and washed with a mixture of $H_2O$/EtOH and stored at room temperature for further characterizations. (Yield = 54 % based on Cu). A schematic of the reaction set up is shown in ESI (Figure S29 in the Supporting Information). A similar synthetic approach was employed for the preparation of all the compounds and the synthetic conditions and composition are presented in Table 4.

**Catalysis:** In a 5 mL flask, aromatic aldehyde (0.5 mmol) and MeOH (2.5 mL) were taken and stirred for 10 minutes. To this mixture, 1.5 mmol of nitromethane (80 µL) and 10 mol% of the catalyst (10 mol %) were added. The entire reaction mixture was kept at 65°C under atmospheric conditions. The progress of the reaction was monitored by employing thin layer chromatography. After the completion of the reaction, the catalyst was separated by filtration and washed with methanol. The filtrate was concentrated employing a rotary evaporator and the crude product was purified by column chromatography (in column chromatography silica gel was taken in the solid phase and hexane / ethyl acetate mixture was employed as the eluent).

**Hot Filtration Studies:** To examine the possible leaching of the catalyst into the reaction mixture, we have carried out the hot filtration test. In the hot filration test, 4-nitrobenzaldehyde (0.5 mmol, 0.076 g), 1.5 mmol of nitromethane (80 µL), catalyst (**III**, 10 mol %) were taken in 2.5 mL MeOH and stirred at 65°C under atmospheric conditions. After 6h the catalyst was removed from the reaction mixture by centrifugation and the yield of the reaction was continuously monitored. The yield was found to be 44 % and after the removal of the catalyst the reaction was continued for 24h. At the end of the reaction, we did not observe any significant increase in the yield of the product (Figure S30 in the supporting information).

**Characterization techniques:**

Initial characterizations were carried out by powder X-ray diffraction (PXRD), infrared spectroscopy (IR), UV–Vis spectroscopy, photoluminescence studies (PL). FTIR spectra were recorded as KBr pellets of the samples on Perkin Elmer L125000P machine using the Spectrum 10$^{TM}$ software. For the compounds (**I-IV**) the broad band at ~ 3200-3480 $cm^{-1}$ represent the presence of water molecules in the structure, the bands ~ 1600 $cm^{-1}$, ~1580 $cm^{-1}$ represents the asymmetric stretching of coordinated $-COO^{-}$ and the C-C stretching of the aromatic ring respectively.[32] Other typical bands have also been observed (Figure S31 in the Supporting Information). Important IR bands have been tabulated (Table S4 in the Supporting Information). The solid state UV−vis absorption spectra of compounds were recorded at room temperature using Perkin Elmer Lambda 35 spectrophotometer. For the compounds (**I-IV**) the band at ~ 406-413 nm observed, which are due to the $\pi-\pi^*$ transition of the ligand (Figure S32, Table S5 in the Supporting Information). The solid state emission study was carried out in PerkinElmer LS 55 luminescence spectrophotometer. The emission spectra were recorded employing the excitation wavelength of 400 nm (Figure S33, Table S5 in the Supporting Information). The emission bands at ~ 443-563 nm are may be due to the $\pi^*-\pi$ transition of the ligand. The bands ~590-649 nm are due to the $[Cu_6(6\text{-}mna)_6]^{6-}$cluster centered transitions mixed with ligand-to-metal charge transfer (LMCT) transitions.[26,55,56]. The PXRD data were recorded in the 2θ range 5–50° using Cu $K_\alpha$ radiation (Philips X'pert). The observed PXRD patterns for all the compounds were found to be consistent with the PXRD patterns simulated from the single crystal structure study (Figure S34 in the Supporting Information). The nitroaldol compounds were characterized by $^1$H-NMR spectroscopy employing a Bruker 400 MHz spectrometer. Chemical shifts in ppm are reported using tetramethylsilane (TMS) as the internal standard.

**Single crystal structure determination:** The single crystal data were collected at 120 K on an Oxford Xcalibur (Mova) diffractometer equipped with an EOS CCD detector. The X–ray generator was operated at 50 kV and 0.8 mA using Mo $K_\alpha$ (λ= 0.71073 Å) radiation. The cell refinement and data reduction were accomplished using CrysAlis RED.[57] The structures were solved by direct methods and refined using SHELX97 present in the WinGX suit of programs (version 1.63.04a).[58] The hydrogen positions were initially located in the difference Fourier map and for the final refinement, the hydrogen positions were fixed in a geometrically ideal position and refined employing riding model. The solvent molecules were found to be disorder in compound **I** and **III** were accounted by using the SQUEEZE option within the WinGX-platon program.[59] The potential solvent accessible voids (for **I** 10.67% and for **III** 9.4% of the total volume of the unit cell) were determined from the SQUEEZE results. The final refinements included atomic positions for all the atoms, anisotropic thermal parameters for all the non–hydrogen atoms except C6 (for **IV**) and isotropic thermal parameters for all the hydrogen atoms. The CCDC numbers for the compounds 1555266 (**I**), 1555267 (**II**), 1555268 (**III**) and 1555269 (**IV**). The details of the structure solution and final refinement parameters are listed in Table 5.

**Table 4.** The synthetic conditions of compounds **I** - **IV**.

| Compound | [{$Zn_3$ (Hen)(OH)}{$Cu_6$(6-mna)$_6$}.($H_2O$)$_6$], (**I**) | [{$Zn_2$(OH)(en)}{$Cu_6$(6-mna)$_6$}$_{0.5}$.($H_2O$)$_2$.EtOH], (**II**) | [{ $Zn_3$(dap)$_3$($H_2$ O)} {$Cu_6$(6-mna)$_6$}. ($H_2O$)$_4$], (**III**) | [{$Zn_2$ (4,4'-bpy)$_{0.5}$(OH)($H_2O$)} {$Cu_6$(6-mna)$_6$ }$_{0.5}$. ($H_2O$)], (**IV**) |
|---|---|---|---|---|
| Compositions | **BL**: Metalloligand (1 mmol) + $H_2O$ (1mL) + en (15 µL)<br>**ML**: [$H_2O$ + EtOH] (1:1) 1mL<br>**TL**: $Zn(NO_3)_2$. $6H_2O$ (0.1 mmol) + EtOH (1mL) | **BL**: Metalloligand (1 mmol) + $H_2O$ (1mL) + en (15 µL)<br>**ML**: [$H_2O$ + EtOH] (1:1) 1mL<br>**TL**: $Zn(OAc)_2$. $2H_2O$ (0.1 mmol) + EtOH (1mL) + $H_2O$ (0.25mL) | **BL**: Metalloligand (1 mmol) + $H_2O$ (1mL) + dap (20 µL)<br>**ML**: [$H_2O$ + EtOH] (1:1) 1mL<br>**TL**: $Zn(NO_3)_2$. $6H_2O$ (0.1 mmol) + EtOH (1mL) | **BL**: Metalloligand (1 mmol) + $H_2O$ (1mL) + $NH_4OH$ (20 µL)<br>**ML**: [$H_2O$ + EtOH] (1:1) 1mL<br>**TL**: $Zn(NO_3)_2$. $6H_2O$ (0.1 mmol) + EtOH (1mL) +4,4'-bpy (1mmol) + DMF (0.5mL) |
| Temp. (°C) | 100 | 100 | 60 | 100 |
| Time (h) | 48 | 96 | 48 | 96 |
| Yield (%) | 54 | 42 | 26 | 76 |

**BL** = bottom layer, **ML** = middle layer, **TL**= top layer, en = ethylenediamine, dap = 1,2-diaminopropane, 4,4'-bpy = 4,4'-bipyridine, DMF **=** N,N'-dimethylformamide.

Elemental analysis: Anal. Calculated (%) for **I**: C 27.35, H 1.57, N 6.72, S 11.53; found: C 25.54, H 1.98, N 6.12, S 11.03; for **II**: C 28.23, H 2.58, N 7.48, S 10.28; found: C 27.22, H 2.95, N 6.87, S 11.14; for **III**: C 30.05, H 2.69, N 9.34, S 10.70; found: C 29.76, H 2.98, N 9.74, S 10.18; for **IV**: C 30.36, H 1.77, N 6.16, S 10.57; found: C 31.14, H 2.18, N 6.77, S 10.49

**Table 5.** Crystal data and structure refinement parameters for **I** - **IV**.

| Structural parameter | **I** | **II** | **III** | **IV** |
|---|---|---|---|---|
| Empirical formula | [{$Zn_3$(Hen)(OH)}{$Cu_6$ (6-mna)$_6$}.($H_2O$)$_6$] | [{$Zn_2$(OH)(en)}{$Cu_6$(6-mna)$_6$}$_{0.5}$.($H_2O$)$_2$.EtOH] | [{$Zn_3$(dap)$_3$($H_2O$)}{$Cu_6$(6-mna)$_6$}.($H_2O$)$_4$] | [{$Zn_2$(4,4'-bpy)$_{0.5}$(OH)($H_2O$)}{$Cu_6$(6-mna)$_6$}$_{0.5}$.($H_2O$)] |
| Formula weight | 1682.60 | 940.10 | 1808.85 | 913.01 |
| Crystal system | Monoclinic | Monoclinic | Triclinic | Triclinic |
| Space group | $P2_1/c$ | $C2/c$ | $P$-1 | $P$-1 |
| a (Å) | 12.8700(5) | 13.9429(3) | 11.1148(5) | 10.4475(5) |
| b (Å) | 20.7985(10) | 19.5452(4) | 16.4516(8) | 11.9018(7) |
| c (Å) | 24.0234(12) | 26.0040(5) | 20.8107(10) | 13.7950(7) |
| α (°) | 90 | 90 | 77.806(4) | 81.153(5) |
| β (°) | 93.165(4) | 98.909(2) | 86.676(4) | 86.546(4) |
| γ (°) | 90 | 90 | 77.019(4) | 64.284(5) |
| V (Å$^3$) | 6420.7(5) | 7001.0(2) | 3624.2(3) | 1527.01(14) |
| Z | 4 | 8 | 2 | 2 |
| T/K | 120 | 120 | 120 | 120 |
| ρ(calc/gcm$^{-3}$) | 1.773 | 1.776 | 1.648 | 1.979 |
| µ (mm$^{-1}$) | 3.307 | 3.376 | 2.935 | 3.864 |
| λ(Mo Kα/Å) | 0.71073 | 0.71073 | 0.71073 | 0.71073 |
| θ range ( °) | 2.52 - 25.00 | 2.55 - 25.00 | 2.51 - 25.00 | 2.50 - 25.00 |
| R indexes [ I > 2σ (I)] | R1 = 0.0676<br>wR2 = 0.1505 | R1 = 0.0340<br>wR2 = 0.0811 | R1 = 0.0644<br>wR2 = 0.1598 | R1 = 0.0631<br>wR2 = 0.1415 |
| R indexes (all data) | R1 = 0.1058<br>wR2 = 0.1727 | R1 = 0.0379<br>wR2 = 0.0832 | R1 = 0.0908<br>wR2 = 0.1764 | R1 = 0.0904<br>wR2 = 0.1572 |

$^aR_1 = \Sigma||F_o| - |F_c||/\Sigma|F_o|$; $wR_2 = \{\Sigma|w(F_o^2 - F_c^2)|/\Sigma [w(F_o^2)^2]\}^{1/2}$. $w = 1/[\rho^2(F_o)^2 + (aP)^2 + bP]$. $P = [\max (F_o{}^{,}O) + 2(F_c)^2]/3$, where a = 0.0679 and b = 0.0000 for **I**, a = 0.0289 and b = 37.0595 for **II**, a = 0.0789 and b = 3.2775 for **III** and a = 0.0605 and b = 1.5764 for **IV**.

## Acknowledgements

The authors thank the Science and Engineering Research Board (SERB), Government of India, for the award of a J. C. Bose National Fellowship. The Council of Scientific and Industrial Research (CSIR), Government of India, is thanked for the award of a research grant (S.N.) and a research fellowship (A.K.J.).

**Keywords:** $Cu_6S_6$ cluster • Zn-oxo cluster • NiAs-related structure • NaCl-related structure • Nitroaldol reaction

[1] M. Hong, *Cryst. Growth Des.* **2007**, *7*, 10−14.

[2] S. Kitagawa, R. Kitaura, S. Noro, *Angew. Chem. Int. Ed.* **2004**, *43*, 2334–2375.

[3] P. J. Hagrman, D. Hagrman, J. Zubieta, *Angew. Chem. Int. Ed.* **1999**, *38*, 2638–2684.

[4] D. Hagrman, R. P. Hammond, R. Haushalter, J. Zubieta, *Chem. Mater.* **1998**, *10,* 2091–2100.

[5] X. Wang, Y. Bi, B. Chen, H. Lin, G. Liu, *Inorg. Chem*. **2008***, 47*, 2442–2448.

[6] J. F. Keggin, *Nature* **1933**, *131*, 908–909.

[7] N. Steunou, G. Kickelbick, K. Boubekeur, C. Sanchez, *J. Chem. Soc. Dalton Trans*. **1999**, 3653–3655.

[8] O. Sadeghi, L. N. Zakharov, M. Nyman, *Science* **2015**, *347*, 1359–1362.

[9] T. Boyd, S. G. Mitchell, D. Gabb, D. L. Long, Y. F. Song, L. Cronin, *J. Am. Chem. Soc*. **2017**, *139*, 5930−5938.

[10] G. Zhang, C. Liu, D. L. Long, L. Cronin, C. H. Tung, Y. Wang, *J. Am. Chem. Soc*. **2016**, *138*, 11097−11100.

[11] R. W. Huang, Y. S. Wei, X. Y. Dong, X. H. Wu, C. X. Du, S. Q. Zang, T. C. W. Mak, *Nature Chemistry* **2017**, *9*, *689−697.*

[12] F. L. Liu, B. Kozlevcar, P. Strauch, G. L. Zhuang, L. Y. Guo, Z. Wang, D. Sun, *Chem. Eur. J*. **2015**, *21*, 18847−18854.

[13] R. G. Pearson, *J. Am. Chem. Soc.* **1963**, *85*, 3533−3539.

[14] H. Ryu, K. M. Park, M. Ikeda, Y. Habata, S. S. Lee, *Inorg. Chem*. **2014**, *53*, 4029−4038.

[15] S. Bhattacharya, M. Gnanavel, A. J. Bhattacharyya, S. Natarajan, *Cryst. Growth Des.* **2014**, *14*, 310−325.

[16] K. Gedrich, I. Senkovska, N. Klein, U. Stoeck, A. Henschel, M. R. Lohe, I. A. Baburin, U. Mueller, S. Kaskel, *Angew. Chem. Int. Ed*. **2010**, *49*, 8489 –8492.

[17] L. Hou, W. X. Zhang, J. P. Zhang, W. Xue, Y. B. Zhanga, X. M. Chen, *Chem. Commun*. **2010**, *46*, 6311–6313.

[18] S. Ma, J. M. Simmons, D. Yuan, J. R. Li, W. Weng, D. J. Liu, H. C. Zhou, *Chem. Commun.* **2009**, 4049–4051.

[19] N. Masciocchi, S. Galli, V. Colombo, A. Maspero, G. Palmisano, B. Seyyedi, C. Lamberti, S. Bordiga, *J. Am. Chem. Soc*. **2010**, *132*, 7902–7904.

[20] D. Sun, D. F. Wang, X. G. Han, N. Zhang, R. B. Huang, L. S. Zheng, *Chem. Commun.* **2011**, *47*, 746–748.

[21] Z. Wang, G. L. Zhuang, Y. K. Deng, Z. Y. Feng, Z. Z. Cao, M. Kurmoo, C. H. Tung, D. Sun, *Inorg. Chem.* **2016**, *55*, 4757−4763.

[22] D. Sun, D. F. Wang, F. J. Liu, H. J. Hao, N. Zhang, R. B. Huang, L. S. Zheng, *CrystEngComm*. **2011**, *13*, 2833–2836.

[23] D. Sun, L. Zhang, H. Lu, S. Feng, D. Sun, *Dalton Trans.* **2013**, *42*, 3528–3532.

[24] D. Sun, L. Zhang, Z. Yan, D. Sun, *Chem. Asian J*. **2012**, *7*, 1558–1561.

[25] A. K. Jana, T. Kundu, S. Natarajan, *Cryst. Growth Des.* **2016**, *16*, 3497–3509.

[26] T. Kundu, A. K. Jana, S. Natarajan, *Cryst. Growth Des.* **2014**, *14*, 4531−4544.

[27] X. C. Shan, F. L. Jiang, D. Q. Yuan, H. B. Zhang, M. Y. Wu, L. Chen, J. Wei, S. Q. Zhang, J. Pan, M. C. Hong, *Chem. Sci.* **2013**, *4*, 1484–1489.

[28] A. A. Ayi, A. Choudhury, S. Natarajan, S. Neeraj, C. N. R. Rao, *J. Mater. Chem.* **2001**, *11*, 1181–1191.

[29] A. Choudhury, S. Neeraj, S. Natarajan, C. N. R. Rao, *J. Mater. Chem.* **2001**, *11*, 1537–1546.

[30] A. Choudhury, S. Neeraj, S. Natarajan, C. N. R. Rao, *J. Mater. Chem.* **2002**, *12*, 1044–1052.

[31] A. Banerjee, P. Mahata, S. Natarajan, *Eur. J. Inorg. Chem.* **2008**, 3501–3514.

[32] K. Nakamoto, Infrared and Raman Spectra of Inorganic and Coordination Compounds: Applications in Coordination, Organometallic, and Bioinorganic Chemistry; Wiley: New York, **2009**, pp. 124-230.

[33] V. A. Blatov, **2006**, http://www.topos.ssu.samara.ru/.

[34] V. A. Blatov, A. P. Shevchenko, V. N. Serezhkin, *J. Appl.Crystallogr*. **2000**, *33*, 1193−1193.

[35] L. O¨hrstro¨m, K. Larsson, Molecule Based Materials, The Structural Network Approach; Elsevier: UK, **2005**.

[36] A.W. Addison, T. N. Rao, *J. Chem. Soc. Dalton Trans.* **1984**, 1349−1356.

[37] A. F. Wells, Structural inorganic chemistry, 5th Edition, Oxford: Clarendon Press, **1984**, pp. 1-1382.

[38] http://www.iza-online.org/

[39] P. Mahata, M. Prabu, S. Natarajan, *Inorg. Chem*. **2008**, *47*, 8451−8463.

[40] I. Tsyba, B. B. Mui, R. Bau, R. Noguchi, K. Nomiya, *Inorg. Chem*. **2003***, 42*, 8028–8032.

[41] B. M. Choudary, M. L. Kantam, C. V. Reddy, K. K. Rao, F. Figueras, *Green Chemistry* **1999**, 187–189.

[42] G. Rosini, R. Ballini, *Synthesis* **1988**, 833–847.

[43] T. Nitabaru, N. Kumagai, M. Shibasaki, *Tetrahedron Letters* **2008**, *49*, 272–276.

[44] T. Risgaard, K. V. Gothelf, K. A. Jørgensen, *Org. Biomol. Chem.* **2003**, *1*, 153–156.

[45] M. N. Kopylovich, A. Mizar, M. F. C. G. D. Silva, T. C. O. M. Leod, K. T. Mahmudov, A. J. L. Pombeiro, *Chem. Eur. J.* **2013**, *19*, 588–600.

[46] H. Naïli, F. Hajlaoui, T. Mhiri, T. C. O. M. Leod, M. N. Kopylovich, K. T. Mahmudov, A. J. L. Pombeiro, *Dalton Trans.* **2013**, *42*, 399–406.

[47] M. N. Kopylovich, T. C. O. M. Leod, K. T. Mahmudov, M. F. C. G. D. Silva*,* A. J. L. Pombeiro, *Dalton Trans.* **2011**, *40*, 5352–5361.

[48] A. Karmakar, M. F. C. G. D. Silva, A. J. L. Pombeiro, *Dalton Trans.* **2014**, *43*, 7795–7810.

[49] Q. T. Nguyen, J. H. Jeong, *Polyhedron* **2008**, *27*, 3227–3230.

[50] J. M. Gu, W. S. Kim, S. Huh, *Dalton Trans.* **2011**, *40*, 10826–10829.

[51] E. Chinnaraja, R. Arunachalam, P. S. Subramanian, *Chemistry Select* **2016**, *1*, 5331–5338.

[52] A. Bulut, A. Aslan, O. Dogan, *J. Org. Chem.* **2008**, *73*, 7373–7375.

[53] B. M. Trost, V.S. C. Yeh, H. Ito, N. Bremeyer, *Org. Lett.* **2002**, *4*, 2621–2623.

[54] B. M. Trost, V.S. C. Yeh, *Angew. Chem. Int. Ed.* **2002**, *41*, 861–863.

[55] V. W. W. Yam, K. K. W. Lo, *Chem. Soc. Rev.* **1999**, *28*, 323–334.

[56] V. W. W. Yam, *Acc. Chem. Res.* **2002,** *35*, 555–563.

[57] CrysAlis CCD, CrysAlis PRO RED, version 1.171.33.34d; Oxford Diffraction Ltd.: Abingdon, Boxfordshire, England, **2009**.

[58] Sheldrick, G. M. SHELXS-97, Program for Crystal Structure Solution and Refinement; University of Go¨ttingen: Go¨ttingen, Germany, **1997**.

[59] P. V. D. Sluis, A. L. Spek, *Acta Cryst.***1990**, *A46*, 194–201.

# FULL PAPER

The molecular $[Cu_6(6\text{-mna})_6]^{6-}$ clusters have been assembled through different Zn-O clusters forming new three-dimensional structures resembling NiAs and NaCl-related structures.

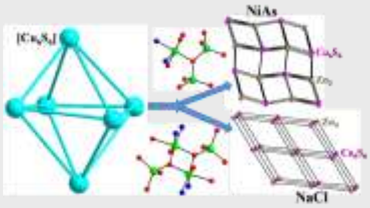

*Ajay Kumar Jana[a] and Srinivasan Natarajan*[a]*

***Page No. – Page No.***

**$Cu_6S_6$ clusters as a building block for the stabilization of coordination polymers with NiAs, NaCl and related structures: synthesis, structure and catalytic studies**